

Article

Development and Validation of an Ultra-Performance Liquid Chromatography-Tandem Mass Spectrometry Method for Quantitative Determination of *N*-((3*S*,4*S*)-4-(3,4-Difluorophenyl)piperidin-3-yl)-2-fluoro-4-(1-methyl-1*H*-pyrazol-5-yl)benzamide in Dog Plasma

Li Ping ¹, Xinwei Dong ¹, Minjuan Zuo ², Yawen Hong ¹ and Difeng Zhu ^{1,*} 

¹ Center for Drug Safety Evaluation and Research of Zhejiang University, College of Pharmaceutical Sciences, Zhejiang University, Hangzhou 310058, China; Pingli552@zju.edu.cn (L.P.); dxw826@zju.edu.cn (X.D.); hongyawen61@zju.edu.cn (Y.H.)

² Hangzhou Leading Pharmatech CO., Ltd., Hangzhou 310058, China; zuomj2016@ldiscover.com.cn

* Correspondence: Zhudf@zju.edu.cn; Tel.: +86-1538-118-2017

Abstract: The PI3K/AKT/MTOR signalling pathway plays an important role in the growth and proliferation of tumour cells. *N*-((3*S*,4*S*)-4-(3,4-Difluorophenyl)piperidin-3-yl)-2-fluoro-4-(1-methyl-1*H*-pyrazol-5-yl)benzamide (Hu7691) is a new-generation selective AKT inhibitor developed at Zhejiang University. In this study, we developed an ultra-performance liquid chromatography-tandem mass spectrometry (UPLC-MS/MS) for the measurement of Hu7691 in dog plasma. Plasma was precipitated with acetonitrile and then separated on a trifunctionally bonded alkyl column. Excellent separation efficiency and selectivity were achieved by adjusting the mobile phase ratio, with a total running time of only 5 min. The linear dynamic range of the calibration curve was 5–1000 ng/mL. The method was fully validated, and all performance metrics met the criteria. The validated method was used for the pharmacokinetic monitoring and bioavailability assessment of Hu7691 in dogs. The results showed that the area under the curve and peak plasma concentration of Hu7691 increased with increasing dose (oral 5, 10, 20 mg/kg, intravenous 10 mg/kg), and oral bioavailabilities were 86.7%, 50.8%, and 50.5%, respectively, indicating a high bioavailability of Hu7691 in dogs. This provides a test basis for the clinical application of the compound.

Keywords: Hu7691; UPLC-MS/MS; dog plasma; pharmacokinetics



Citation: Ping, L.; Dong, X.; Zuo, M.; Hong, Y.; Zhu, D. Development and Validation of an Ultra-Performance Liquid Chromatography-Tandem Mass Spectrometry Method for Quantitative Determination of *N*-((3*S*,4*S*)-4-(3,4-Difluorophenyl)piperidin-3-yl)-2-fluoro-4-(1-methyl-1*H*-pyrazol-5-yl)benzamide in Dog Plasma. *Appl. Sci.* **2022**, *12*, 158. <https://doi.org/10.3390/app12010158>

Academic Editor: Emilio Martines

Received: 19 October 2021

Accepted: 14 December 2021

Published: 24 December 2021

Publisher's Note: MDPI stays neutral with regard to jurisdictional claims in published maps and institutional affiliations.



Copyright: © 2021 by the authors. Licensee MDPI, Basel, Switzerland. This article is an open access article distributed under the terms and conditions of the Creative Commons Attribution (CC BY) license (<https://creativecommons.org/licenses/by/4.0/>).

1. Introduction

The phosphatidylinositol 3-kinase (PI3K)/protein kinase B (also known as AKT)/mammalian target of rapamycin (MTOR) pathway plays an important role in the growth and proliferation of tumour cells [1]. Clinical data indicate that this signalling pathway is abnormally activated in more than 30% of malignant tumours. Meanwhile, numerous data show that the inhibition of this signalling pathway can effectively inhibit tumour growth. Therefore, targeting the key protein molecules of the PI3K/AKT/MTOR signalling pathway has attracted increased attention in the research and development of new antitumour drugs.

AKT is a general name for three subtypes of serine/threonine protein kinases, AKT1, AKT2, and AKT3 [2], which are closely related to and play a significant role in regulating the growth, proliferation, survival, and metabolism of cells. PI3K activation generates phosphatidylinositol (3,4,5)-trisphosphate (PIP₃), which interacts with the pleckstrin homology (PH) domain of AKT, resulting in its translocation and conformational changes. After PIP₃ binds to the PH domain of AKT, PDK1 and PDK2 phosphorylate; AKT is activated only after both are phosphorylated. The activated AKT is transferred from the cell membrane to the cytoplasm or nucleus, where it targets and regulates, via phosphorylation, downstream signalling molecules, such as MTOR, BAD, and cyclin D1, to promote cell growth and

inhibit apoptosis. Therefore, AKT is the core protein in the PI3K/AKT/MTOR signalling pathway. It can inhibit tumour cell apoptosis and promote tumour cell survival [3–5]. It can also promote the tumour cell cycle, which results in tumour cell overproliferation [5–7].

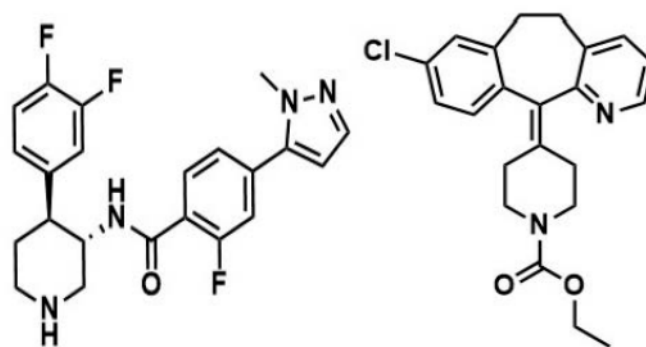
With increasing insights into the structure, function, and mechanism of action of AKT, the application of small-molecule AKT inhibitors in the field of antitumour therapy has received increasing attention, and numerous structural types of small-molecule AKT inhibitors have been reported [8,9]. Since 2000, more than 10 AKT inhibitors, such as perifosine, triciribine, GSK690693, XL418, and UCN-01, have entered clinical trials. However, most of the developed AKT-specific antitumour therapy candidate compounds show problems such as a poor stability, poor cell permeability, and poor solubility.

N-((3*S*,4*S*)-4-(3,4-Difluorophenyl)piperidin-3-yl)-2-fluoro-4-(1-methyl-1*H*-pyrazol-5-yl)benzamide (Hu7691) is a new-generation selective AKT inhibitor, which was independently developed at Zhejiang University [10]. Hu7691 was systematically optimised via molecular docking and rational drug design, mainly to overcome the problems of poor kinase selectivity and hERG channel blockade by AKT inhibitors. Consequently, improved kinase selectivity and improved *in vitro* and *in vivo* efficacy and safety were achieved. Nevertheless, no studies have reported the detection methods used in biological samples from Hu7691. In this study, a novel UPLC-MS/MS method for bioanalysis of Hu7691 in dog plasma was established, validated, and applied to pharmacokinetic monitoring and bioavailability assessment in beagles. The data of this study may be used for future preclinical and clinical evaluation of this compound.

2. Materials and Methods

2.1. Chemicals and Materials

Hu7691 (99.5% purity) was sourced from the Institute of Innovative Medicine, Zhejiang University (Hangzhou, China). Loratadine (100.0% purity), the internal standard (IS), was provided by the National Institutes for Food and Drug Control of China (Beijing, China). Methanol and acetonitrile were purchased from Merck (Darmstadt, Germany). Formic acid was purchased from Sigma–Aldrich (St. Louis, MO, USA). Milli-Q water (18.2 MΩ-cm) was prepared using a Purelab OptionS7 ultrapure water system (ELGA LabWater, UK). The structures of Hu7691 and IS are illustrated in Figure 1.



Hu7691 Loratadine

Figure 1. Chemical structures of Hu7691 and loratadine.

2.2. Animal Experimentation

The animal experimental protocol was approved by the Animal Experimental Committee of the Center for Drug Safety Evaluation and Research, Zhejiang University. Beagle dogs were purchased from Jiangsu Yadong Laboratory Animal Research Institute Co., Ltd. (Nanjing, China). The animal research complied with the principles of the 3Rs (Reduction, Replacement, and Refinement).

2.3. Instrumentation and Conditions

The UPLC system was an ACQUITY UPLC I-Class system (Waters Corporation, MA, USA) with an ACQUITY UPLC BEH C18 chromatographic column (2.1 × 100 mm, 1.7 μm). The column temperature was set to 40 °C. The mobile phase consisted of acetonitrile and 0.1% formic acid water at a flow rate of 0.300 mL/min. Gradient elution was performed as follows: 0.00–0.50 min, 10% B; 0.50–1.50 min, 10–90% B; 1.50–3.50 min, 90% B; 3.50–3.51 min, 90–10% B; 3.51–5.00 min, 10% B. The injection volume was 1 μL.

The mass spectrometer was set to negative multiple reaction monitoring (MRM) mode, Hu7691 was detected using a parent ion m/z of 415.11 and a daughter ion m/z of 196.09 under a fragmentation voltage of 5 V and a collision energy of 22 eV, and loratadine was detected using a parent ion m/z of 383.08 and a daughter ion m/z of 267.02 under 5 V and 32 eV. The optimised MS/MS parameters are as follows: capillary voltage, 3.00 kV; ion source temperature, 150 °C; desolvation gas temperature, 350 °C; collision gas flow rate, 0.15 mL/min; and desolvation gas flow rate, 650 L/h.

2.4. Sample Preparation

Six times the volume of acetonitrile was used to precipitate the proteins in the plasma sample. Plasma samples (50 μL) were mixed with 300 μL of acetonitrile (containing 4 ng/mL loratadine as the internal standard), then vortexed for 10 min and centrifuged at 12,000 rpm for 10 min. The supernatant was separated and recentrifuged at 12,000 rpm for 5 min to improve the purity, followed by injecting aliquots of the supernatant into the LC system.

2.5. Method Validation

Method validation was performed following the Bioanalytical Method Validation.

Guidance for Industry [11]. The following performance metrics of the method were examined: specificity, lower limit of detection, lower limit of quantification (LLOQ), linearity, precision and accuracy, recovery, matrix effect (ME), and so on [12].

2.5.1. Preparation of Standard and Quality Control (QC) Samples

Stock solutions of Hu7691 and loratadine were prepared in methanol. Standard curve samples of Hu7691 were prepared in rat blank plasma at concentrations of 5, 10, 20, 50, 100, 200, 500, and 1000 ng/mL.

QC samples were prepared at 5, 15, 400, 800 ng/mL concentrations in the plasma and were stored at −20 °C until analysis.

2.5.2. Specificity, Linearity, LLOD, and LLOQ

The specificity of potential interference was studied by comparing three chromatograms of blank plasma from six beagles, blank plasma with Hu7691 and IS added, and plasma samples from Hu7691 2 h after administration.

To assess the linearity, a series of plasma working solutions containing from 5 to 1000 ng/mL Hu7691 were prepared. The peak area ratio of Hu7691 to loratadine was counted, and the calibration curve was obtained by plotting the peak area ratio vs. LLOD, the lowest detectable concentration of the analyte in samples was calculated as a signal-to-noise (S/N) ratio > 3. LLOQ, the lowest quantifiable concentration of the analyte in samples, was calculated as a signal-to-noise (S/N) ratio > 10.

2.5.3. Recovery and ME

Recovery determination was obtained by comparing the peak area ratios of three QC samples with those of spiked, post-extraction blank samples (three samples per concentration). The recovery was acquired by comparing the response of the extracted sample with the blank plasma spiked extract sample.

The ME was measured by comparing the peak areas of Hu7691 pure solution samples at three QC concentrations (six samples per concentration). The ME was determined by contrasting the ratio between the post-extracted blank samples and the unextracted sample.

2.5.4. Inter- and Intra-Assay Precision and Accuracy

Accuracy and precision were measured by the performance of QC samples (five samples per concentration) with three batches. The inter- and intra-assay precision were required to be within 15%, and accuracy within the range of 85–115%, while the LLOQ samples must be $\leq 20\%$ or within 80–120%.

2.5.5. Stability

For stability evaluation, the Hu7691 and loratadine stock solutions were stored in a refrigerator (2–8 °C) for 7 days. In addition, plasma samples spiked with Hu7691 were stored under the following conditions: in ice boxes for 4 h, in an autosampler for 12 h after sample processing, frozen at –16 to –24 °C for 15 days and then thawed, or subjected to three freeze-thaw cycles.

2.5.6. Dilution Reliability and Residue Verification

Some sample concentrations were beyond the highest point of the standard. The dilution factors of Hu7691 were 10 and 50, with accuracy and precision within 15%.

Residues were assessed by checking the upper limit of standard curves and blank plasma samples. The responses detected in blank samples must be $< 20\%$ of the LLOQ, with accuracy and precision within 15%.

2.6. PK

Twenty-four beagle dogs were randomised into four groups ($n = 6$, each group containing 3 male and 3 female dogs). The Hu7691 were orally administered at a dose of 5, 10, and 20 mg/kg groups, respectively, and at a dose of 10 mg/kg to the intravenous injection group.

Blood samples (0.5 mL) were gathered into heparinised tubes from the lateral small saphenous vein of the right hind limb at the following time points: pre-dose (0 min), 30 min, 1 h, 2 h, 4 h, 6 h, 8 h, 10 h, 24 h, 48 h, 72 h, and 96 h after oral administration. For the intravenous group as following time points: pre-dose (0 min), 15 min, 30 min, 1 h, 2 h, 4 h, 8 h, 24 h, 30 h, 48 h and 72 h. After centrifugation at 3000 rpm for 10 min, samples were transferred and frozen at –20 °C before analysis.

2.7. Statistical Analysis

Data processing and statistical calculations were carried out by Microsoft Office Excel 2007 and SPSS Statistics 19.0. The main pharmacokinetic parameters were computed using a noncompartmental model by the Data Analysis System software version 3.1.

3. Results and Discussion

3.1. Optimisation of the UPLC-MS/MS Method

Due to the similar molecular weight, similar chromatographic behaviour, and corresponding characteristics, loratadine was chosen as the IS without interfering with the detected Hu7691. Hu7691 and Loratadine (IS) are more sensitive and stable than negative electrospray ionisation under positive electrospray ionisation. The full scan spectra of Hu7691 and Loratadine mainly produce protonated ion $[M + H]^+$ at m/z 415.11 and m/z 383.08, respectively. The major fragment ions of its products were at m/z 196.09 and m/z 267.02. Therefore, the MRM mode was acquired using the ion transitions of m/z 415.11 \rightarrow 196.09 for Hu7691 and m/z 383.08 \rightarrow 267.02 for the IS. Other MS detection conditions were also optimised. The optimisation results are displayed in Table 1.

Table 1. Mass spectrometry detection conditions for Hu7691 and IS.

Analyte	Precursor Ion, <i>m/z</i>	Product Ion, <i>m/z</i>	Cone Voltage, V	Collision Energy, eV
Hu7691	415.11	196.09	5	22
Loratadine	383.08	267.02	5	32

Various UPLC columns with different particle sizes, apertures, and column lengths were selected. The ACQUITY UPLC BEH C18 trifunctionally bonded alkyl column was selected after preliminary tests because the target compounds showed acceptable chromatographic peak shapes. Meanwhile, elution methods were screened using methanol, acetonitrile, or isopropanol and formic acid, ammonium formate, or ammonium acetate in water as the mobile phase. The data showed that the use of acetonitrile and 0.1% formic acid could improve the separation of the analytes. The retention times of Hu7691 and loratadine were 1.91 and 2.28 min, respectively.

3.2. Optimisation of Sample Preparation

Biological sample preparation can be achieved using various methods, which mainly include protein precipitation [13,14], enzymatic hydrolysis [15], and extraction [16,17]. Given low *in vivo* concentrations of analytes, sample preparation methods should maximally eliminate the interference of impurities to ensure that the recovery of each component is at an acceptable range. Methanol precipitation, acetonitrile precipitation, and ethyl acetate extraction were compared. Acetonitrile precipitation was finally selected as the sample preparation method, as it achieved a high Hu7691 recovery.

3.3. Method Validation

The calibration curve of Hu7691 showed excellent linearity in the range of 5–1000 ng/mL. Each performance metric of the analysis method of Hu7691 was in an acceptable range, with the intra- and interday precision and accuracy being within acceptable limits [11].

3.3.1. Specificity, Linearity, LLOD, and LLOQ

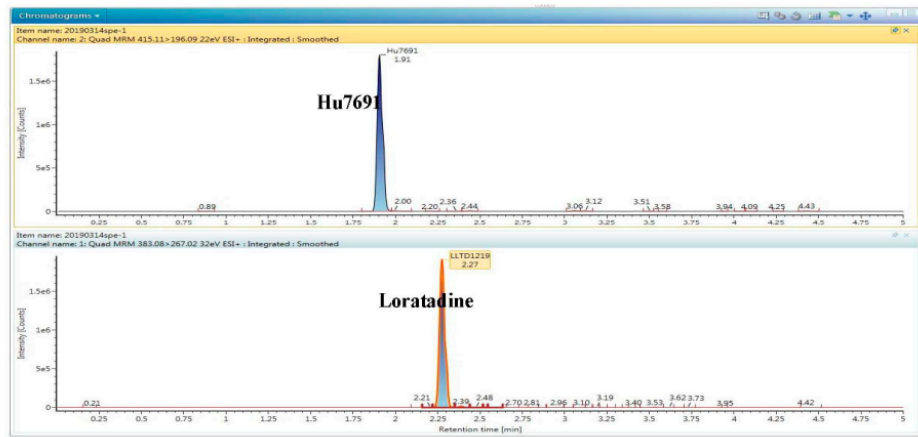
The satisfactory specificity of an analytical method shows that the method may distinguish between the compound and other interfering substances. As demonstrated by the following chromatograms (Figure 2), the blank biological samples did not show interfering signals near the retention times of Hu7691 and loratadine, and the two analytes were well separated, indicating a satisfactory specificity of the method.

The linearity of the standard curve (Figure 3) was assessed by the squared coefficient of correlation (R^2). The R^2 values were all above 0.99, and the typical calibration curve equation for plasma Hu7691 was $y = 5.65 \times 10^4 x - 7.64 \times 10^3$ with $r = 0.995178$, indicating a good linearity.

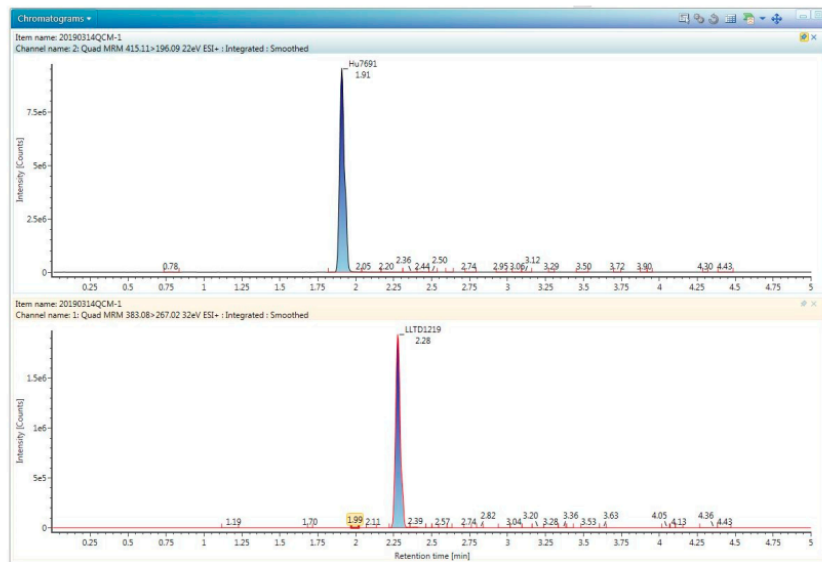
The LLOQ of Hu7691 was 5 ng/mL [RSD = 6.9%, $n = 5$, signal-to-noise ratio (S/N) > 10], and the LLOD was 2 ng/mL ($n = 5$, S/N > 3).

3.3.2. Recovery, ME, and Intra- and Interday Precision

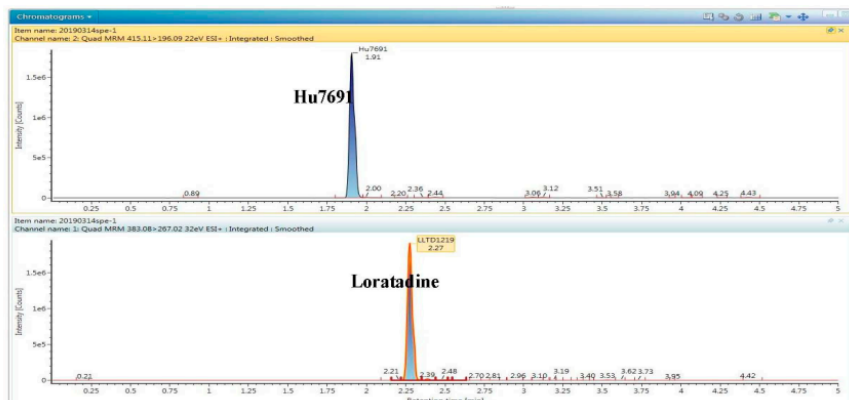
The recovery and ME ranged for Hu7691 from 96.7 to 98.5% and 96.1 to 105.1%, separately. The precision values were both less than 10%, as summarised in Table 2.



(a)



(b)



(c)

Figure 2. Typical UPLC-MS/MS chromatograms of (a) blank plasma; (b) blank plasma spiked with Hu7691 at LLOQ; and (c) an actual sample acquired from a dog 2 h after gavaging Hu7691.

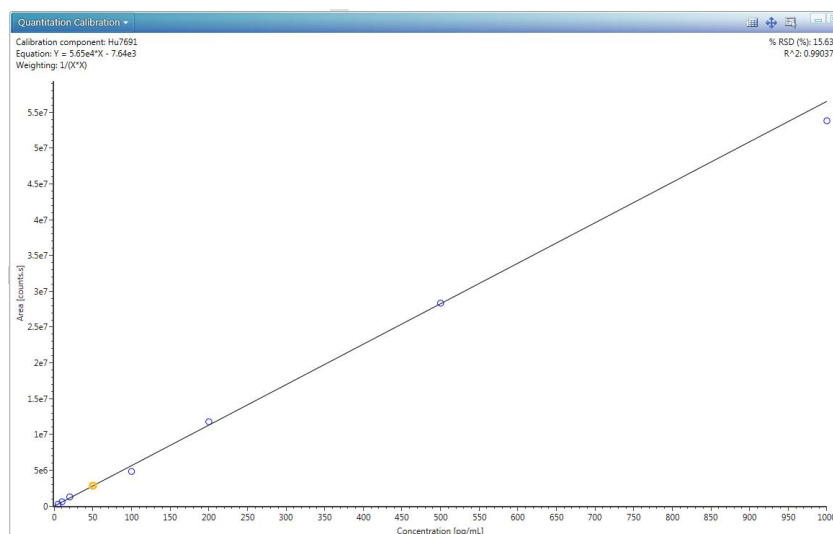


Figure 3. Linear fitting equation of the Hu7691 signal versus concentration.

Table 2. Inter- and intra-assay precision and accuracy of Hu7691 in beagles (n = 5).

Hu7691 Concentration (ng/mL)	Intraday			Interday		
	Mean ± SD	Precision (%)	Accuracy (%)	Mean ± SD	Precision (%)	Accuracy (%)
5	4.9 ± 0.3	6.9	97.7	5.2 ± 0.1	1.8	104.0
15	14.7 ± 0.4	2.5	98.0	15.1 ± 0.9	6.0	100.4
400	394.7 ± 4.1	1.1	98.7	423.6 ± 23.2	5.5	105.9
800	1478.9 ± 11.9	1.4	106.1	834.1 ± 33.9	4.1	104.3

SD, standard deviation.

3.3.3. Sample Stability, Dilution Reliability, and Residues in the Instrument

The Hu7691 and loratadine signals were stable, varying by 4.13–5.78% after their stock solutions were frozen at 2–8 °C in a refrigerator for seven days. Moreover, Hu7691 signals remained stable in plasma placed in ice boxes for 4 h, processed plasma placed in the autosampler for 12 h, plasma subjected to three freeze-thaw cycles and frozen at −16 to −24 °C for 15 days (Table 3). These findings indicate that Hu7691 is stable under the above conditions.

Table 3. Stability of Hu7691 (n = 3).

Spiked Concentration (ng/mL)	4 h (Ice)		12 h (Autosampler)		15 Days (−16 to −24 °C)		Freeze-Thaw Cycles (×3)	
	Mean ± SD	Accuracy (%)	Mean ± SD	Accuracy (%)	Mean ± SD	Accuracy (%)	Mean ± SD	Accuracy (%)
15	16.2 ± 1.3	107.6	16.3 ± 0.6	108.8	13.9 ± 0.2	93.1	15.8 ± 1.7	105.3
800	804.5 ± 17.4	100.6	865.3 ± 10.9	108.2	735.9 ± 23.7	91.9	726.3 ± 4.6	90.8

The accuracy and precision of Hu7691 determination in diluted samples were within ±15%, showing that Hu7691-spiked plasma samples were steady after dilution by a factor of 10 or 50. The residual Hu7691 concentrations in the blank plasma samples after measuring spiked plasma samples at the upper limit concentration of the calibration curve were not greater than 20% of the LLOQ, indicating that the residual concentration of Hu7691 in the instrument was acceptable.

3.4. Pharmacokinetic Study in Dogs

Plasma samples from a total of 24 dogs were analysed using the validated UPLC-MS/MS detection method to investigate the pharmacokinetic changes of Hu7691 in dogs. The main pharmacokinetic parameters, including the area under the curve (AUC_{0–t}), peak

plasma concentration (C_{max}), and elimination half-life ($T_{1/2}$), are displayed in Table 4. As the concentration vs. time curves show (Figure 4), the absolute bioavailability of Hu7691 in dogs treated orally with the low, medium, and high doses of Hu7691 were 86.7%, 50.8%, and 50.5%, respectively. The AUC and C_{max} of Hu7691 in the dog plasma increased with the increasing dose. For oral administration, the in vivo bioavailability was considerably higher at the low dose than at the medium and high doses.

Table 4. Pharmacokinetic parameters of Hu7691 in dogs.

Dose (mg/kg)	C_{max} (ng/mL)	$T_{1/2}$ (h)	MRT_{0-t} (h)	AUC_{0-t} (ng·h/mL)	$AUC_{0-\infty}$ (ng·h/mL)	F (%)
5 (p.o.)	248.2 ± 49.3	34.3 ± 20.4	28.8 ± 7.8	7850 ± 2473	10389 ± 5049	86.7
10 (p.o.)	302.5 ± 94.0	25.0 ± 4.9	26.7 ± 2.6	9189 ± 3955	9785 ± 4142	50.8
20 (p.o.)	415.9 ± 152.0	37.2 ± 18.3	34.6 ± 6.9	18289 ± 4099	22174 ± 4229	50.5
10 (i.v.)	456.1 ± 90.8	29.4 ± 13.9	25.3 ± 4.2	18099 ± 6980	23428 ± 12786	—

C_{max} , peak plasma concentration; $T_{1/2}$, elimination half-life; MRT , mean residence time; AUC , area under the curve; F , fraction absorbed (bioavailability); p.o., per os; i.v., intravenous.

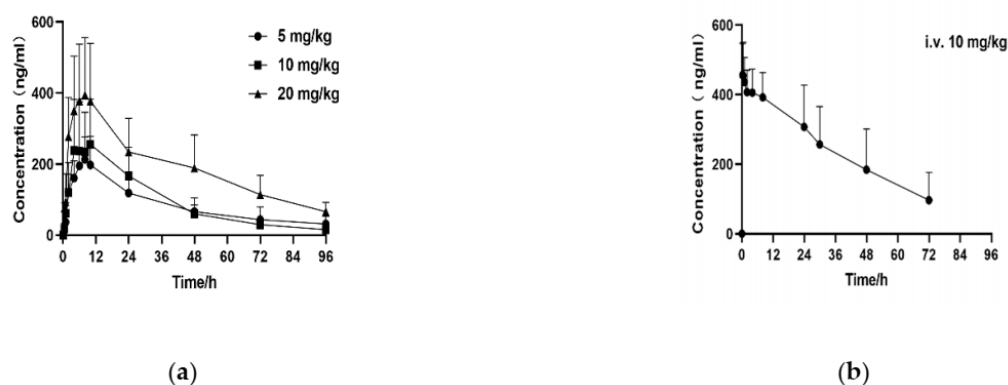


Figure 4. Mean plasma concentration-time curves of Hu7691 in beagles following (a) oral administration and (b) intravenous administration.

4. Conclusions

In summary, we developed and validated an UPLC-MS/MS assay for the quantitation of Hu7691 in dog plasma, which was characterised by good selectivity, high separation efficiency, and fast operation. This bioanalytical method was validated by examining its linearity, precision, and stability. The LOQ ranged from 5 to 1000 ng/mL. We then successfully employed this method to study the pharmacokinetics of Hu7691 in beagles. The results showed that Hu7691 had a high bioavailability in dogs and that the AUC and C_{max} of Hu7691 in dog plasma increased with the increasing dose. The research achievement indicated that Hu7691 had high gastrointestinal absorption and stable pharmacokinetic characteristics and was suitable for oral administration. This study is the first to investigate the pharmacokinetics of Hu7691 in beagles, the findings of this research are essential for further development of Hu7691 and provide a valuable reference for the clinical application of this compound.

Author Contributions: Conceptualisation, D.Z.; methodology and software, X.D. and M.Z.; validation, Y.H. and L.P.; writing—original draft preparation, L.P.; writing—review and editing, D.Z.; funding acquisition, D.Z. All authors have read and agreed to the published version of the manuscript.

Funding: This research received no external funding.

Institutional Review Board Statement: This study was approved by the Institutional Animal Care and Use Committee of the Center for Drug Safety Evaluation and Research of Zhejiang University (IACUC-19-010).

Informed Consent Statement: Not available.

Data Availability Statement: The data that support the findings of this research are available on request from the corresponding author and are not publicly available due to confidentiality reasons.

Conflicts of Interest: The authors declare no conflict of interest.

References

1. Thorpe, L.M.; Yuzugullu, H.; Zhao, J.J. PI3K in cancer: Divergent roles of isoforms, modes of activation and therapeutic targeting. *Nat. Rev. Cancer* **2015**, *15*, 7–24. [[CrossRef](#)] [[PubMed](#)]
2. Engelman, J.A.; Chen, L.; Tan, X.; Crosby, K.; Guimaraes, A.R.; Upadhyay, R.; Maira, M.; McNamara, K.; Perera, S.A.; Song, Y.; et al. Effective use of PI3K and MEK inhibitors to treat mutant *Kras* G12D and *PIK3CA* H1047R murine lung cancers. *Nat. Med.* **2008**, *14*, 1351–1356. [[CrossRef](#)] [[PubMed](#)]
3. Johnstone, R.W.; Ruefli, A.A.; Lowe, S.W. Apoptosis: A link between cancer genetics and chemotherapy. *Cell* **2002**, *108*, 153–164. [[CrossRef](#)]
4. del Peso, L.; Gonzalez-Garcia, M.; Page, C.; Herrera, R.; Nuñez, G. Interleukin-3-induced phosphorylation of BAD through the protein kinase Akt. *Science* **1997**, *278*, 687–689. [[CrossRef](#)] [[PubMed](#)]
5. Kitada, S.; Krajewska, M.; Zhang, X.; Scudiero, D.; Zapata, J.M.; Wang, H.G.; Shabaik, A.; Tudor, G.; Krajewski, S.; Myers, T.G.; et al. Expression and location of apoptosis-regulating Bcl-2 family protein BAD in normal human tissues and tumor cell lines. *Am. J. Pathol.* **1998**, *152*, 51–61. [[PubMed](#)]
6. El-Deiry, W.S. Akt takes centre stage in cell-cycle deregulation. *Nat. Cell Biol.* **2001**, *3*, E71–E73. [[CrossRef](#)] [[PubMed](#)]
7. Zhou, B.P.; Liao, Y.; Xia, W.; Spohn, B.; Lee, M.H.; Hung, M.C. Cytoplasmic localization of p21Cip1/WAF1 by Akt-induced phosphorylation in HER-2/neu-overexpressing cells. *Nat. Cell Biol.* **2001**, *3*, 245–252. [[CrossRef](#)] [[PubMed](#)]
8. Lindsley, C.W. The Akt/PKB family of protein kinases: A review of small molecule inhibitors and progress toward target validation: A 2009 update. *Curr. Top. Med. Chem.* **2010**, *10*, 458–477. [[CrossRef](#)] [[PubMed](#)]
9. Mattmann, M.E.; Stoops, S.L.; Lindsley, C.W. Inhibition of Akt with small molecules and biologics: Historical perspective and current status of the patent landscape. *Expert Opin. Ther. Pat.* **2011**, *21*, 1309–1338. [[CrossRef](#)] [[PubMed](#)]
10. Che, J.; Dai, X.; Gao, J.; Sheng, H.; Zhan, W.; Lu, Y.; Li, D.; Gao, Z.; Jin, Z.; Chen, B.; et al. Discovery of *N*-((3*S*,4*S*)-4-(3,4-difluorophenyl)piperidin-3-yl)-2-fluoro-4-(1-methyl-1*H*-pyrazol-5-yl)benzamide (Hu7691), a potent and selective Akt inhibitor that enables decrease of cutaneous toxicity. *J. Med. Chem.* **2021**, *64*, 12163–12180. [[CrossRef](#)] [[PubMed](#)]
11. Bioanalytical Method Validation Guidance for Industry; U.S. Department of Health and Human Services; Food and Drug Administration; Center for Drug Evaluation and Research (CDER); Center for Veterinary Medicine (CVM). Food and Drug Administration Guidance for Industry: Bioanalytical Method Validation. May 2018. Available online: <https://www.fda.gov/regulatory-information/search-fda-guidance-documents/bioanalytical-method-validation-guidance-industry> (accessed on 4 August 2020).
12. Ping, L.; Xu, B.; Zhou, Q.; Hong, Y.; Sun, Q.; Wang, J.; Zhu, D. Comparative Pharmacokinetic Study of Forchlorfenuron in Adult and Juvenile Rats. *Molecules* **2021**, *26*, 4276. [[CrossRef](#)] [[PubMed](#)]
13. Rehm, S.; Rentsch, K.M. A 2D HPLC-MS/MS method for several antibiotics in blood plasma, plasma water, and diverse tissue samples. *Anal. Bioanal. Chem.* **2020**, *412*, 715–725. [[CrossRef](#)] [[PubMed](#)]
14. Yu, Y.; Liu, H.; Tu, M.; Qiao, M.; Wang, Z.; Du, M. Mass spectrometry analysis and in silico prediction of allergenicity of peptides in tryptic hydrolysates of the proteins from *Ruditapes philippinarum*. *J. Sci. Food Agric.* **2017**, *97*, 5114–5122. [[CrossRef](#)] [[PubMed](#)]
15. Lu, X.; Zhang, L.; Sun, Q.; Song, G.; Huang, J. Extraction, identification and structure-activity relationship of antioxidant peptides from sesame (*Sesamum indicum* L.) protein hydrolysate. *Food Res. Int.* **2019**, *116*, 707–716. [[CrossRef](#)] [[PubMed](#)]
16. Li, Y.; Sun, M.; Mao, X.; Li, J.; Sumarah, M.W.; You, Y.; Wang, Y. Tracing major metabolites of quinoxaline-1,4-dioxides in abalone with high-performance liquid chromatography tandem positive-mode electrospray ionisation mass spectrometry. *J. Sci. Food Agric.* **2019**, *99*, 5550–5557. [[CrossRef](#)] [[PubMed](#)]
17. Zhang, X.; Wang, J.; Wu, Q.; Li, L.; Wang, Y.; Yang, H. Determination of kanamycin by high performance liquid chromatography. *Molecules* **2019**, *24*, 1902. [[CrossRef](#)] [[PubMed](#)]